

# Analysis of hurricane directionality effects using event-based simulation

Zhigang Huang<sup>†</sup>

*Applied Research Associates, Raleigh, NC, U.S.A.*

David V. Rosowsky<sup>‡</sup>

*Forest Products and Civil Engineering, Oregon State University, Corvallis, OR 97331-5751, U.S.A.*

**Abstract.** This paper presents an approach for evaluating directionality effects for both wind speeds and wind loads in hurricane-prone regions. The focus of this study is on directional wind loads on low-rise structures. Using event-based simulation, hurricane directionality effects are determined for an open-terrain condition at various locations in the southeastern United States. The wind speed (or wind load) directionality factor, defined as the ratio of the  $N$ -year mean recurrence interval (MRI) wind speed (or wind load) in each direction to the non-directional  $N$ -year MRI wind speed (or wind load), is less than one but increases toward unity with increasing MRI. Thus, the degree of conservatism that results from neglecting directionality effects decreases with increasing MRI. It may be desirable to account for local exposure effects (siting effects such as shielding, orientation, etc.) in design. To account for these effects in a directionality adjustment, the factor described above for open terrain would need to be transformed to other terrains/exposures. A “local” directionality factor, therefore, must effectively combine these two adjustments (*event* directionality and *siting* or *local exposure* directionality). By also considering the direction-specific aerodynamic coefficient, a direction-dependent wind load can be evaluated. While the data necessary to make predictions of directional wind loads may not routinely be available in the case of low-rise structures, the concept is discussed and illustrated in this paper.

**Key words:** directionality; hurricane; probability; simulation; wind load; wind speed.

---

## 1. Introduction

The extreme wind climate at any given site exhibits directional dependence due to basic atmospheric flow patterns as well as local exposure effects (Simiu and Scanlan 1996). Furthermore, because of the directionality effects on aerodynamic pressure coefficients and the dynamic response of structures, the wind effects on structures are also direction-dependent. Taking into account directionality effects may offer economic benefits in the design of certain structures, e.g., when the predominant extreme wind direction and least favorable structural orientation (and hence aerodynamic coefficients) do not coincide. Directionality effects for non-hurricane and hurricane-prone regions have been addressed previously (Davenport 1977, Simiu and Filliben 1981, Wen 1983, 1984, Simiu and Scanlan 1996, Simiu and Heckert 1998). However, the focus of these studies has been on the directionality of wind

---

<sup>†</sup> Senior Engineer

<sup>‡</sup> Professor and Richardson Chair in Wood Engineering/Mechanics

loads without specific consideration of effects due to atmospheric flow and local exposure, i.e., the factors affecting wind speed directionality. Since the directionality of wind loads also depends on the pressure coefficients, and thus are structure-specific, the findings from these studies cannot be generalized to other locations or structural types. Event-based simulation (e.g., Huang *et al.* 1999) can be used in an analysis to separate out directionality effects due to atmospheric flow, local exposure, and aerodynamic pressure coefficients. By considering these effects separately, the results may be able to be extended to other sites assuming that the exposures are characterized realistically. The focus in this study is on directionality effects on low-rise structures in hurricane-prone regions. As such, no attempt is made to characterize wind directionality effects in non-hurricane-prone regions.

Two approaches can be used in a statistical analysis of (e.g., annual extreme) wind records to determine appropriate nominal wind speeds for use in structural design. *Directional* methods consider the directional dependence of both the wind speeds and the wind loads (functions of the wind speeds and appropriate aerodynamic coefficients). *Non-directional* (or *direction-independent*) methods consider the maximum wind speeds irrespective of direction. These are then used with direction-independent (i.e., worst-case) aerodynamic coefficients in design. Non-directional analysis is the basis for the values found on basic wind maps in most codes and standards in the U.S. (in some cases these are adjusted to account, in a very approximate way, for directionality). Besides being simpler, this approach has been assumed to result in conservative design wind speeds.

## 2. Hurricane wind field model and Monte Carlo simulation

A number of models have been adopted for use in hurricane wind speed simulations and risk analysis studies (Russell 1968, 1971, Tryggvason *et al.* 1976, Batts *et al.* 1980, Tuleya *et al.* 1984, Georgiou 1985, Vickery and Twisdale 1995). Huang (1999) evaluated and compared a number of these models using data from hurricanes Hugo, Fran, Bonnie, Earl, and Georges. In general, Batts' model was found to overestimate the surface wind speeds, while Georgiou's model was found to predict the surface wind speeds quite well at inland sites and at sites close to the ocean when the wind was blowing from the ocean. However, Georgiou's model overpredicted the wind speeds at sites near the coast and underpredicted the gradient wind speeds in the region of most intense winds, i.e., the eye wall. To overcome these problems, Georgiou's model was modified by Huang (1999) to be able to better predict wind speeds. Specifically, a modification factor was applied to the models estimate of the gradient wind speed. The modification factor is a function of the central pressure difference ( $\Delta P$ ), the radius of maximum winds ( $R_m$ ), and the translational wind speed ( $V_t$ ), as well as the relative distance to the hurricane center ( $r/R_m$ ). Surface wind speeds were then obtained by reducing the gradient wind speed in a manner appropriate for the terrain, and rotating the wind direction counterclockwise, also by an amount related to the terrain roughness (typically 15°-20° over water and 30°-40° over land) (*see* Huang 1999). The modified Georgiou's model was used in the simulation in this study. While the probability-based wind field model is not the focus of this paper, the interested reader can find further details of this model elsewhere (Huang *et al.* 1998, Huang 1999, Huang *et al.* 1999).

Once a hurricane makes landfall, the energy balance between the heat source and frictional dissipation is disturbed due to the reduced availability of heat and increased frictional dissipation. This results in a rise in the atmospheric pressure in the storm's center, and consequently, the hurricane weakens and the wind speeds decrease. The rise in the central pressure is most often used to model the weakening of a landfalling hurricane. Based on an analysis of historical hurricanes (*see*

Table 1 Statistics of hurricane model parameters (Huang 1999)

Parameter	Distribution	Distribution parameters			
		North Carolina	South Carolina	Florida (Atlantic Coast)	Florida (Gulf Coast)
Annual occurrence rate, $\lambda$	Poisson	$\lambda = 0.277$	$\lambda = 0.306$	$\lambda = 0.252$	$\lambda = 0.379$
Approach angle, $\theta$ (degrees)	Normal	$\mu = 2.19$ $\sigma = 42.77$	$\mu = -20.88$ $\sigma = 44.41$	$\mu = -60.05$ $\sigma = 24.79$	$\mu = 34.42$ $\sigma = 29.78$
Central pressure difference, $\Delta P$ (mb)	Weibull	$u = 51.120$ $k = 3.155$	$u = 50.094$ $k = 2.304$	$u = 64.831$ $k = 3.465$	$u = 42.751$ $k = 3.929$
Radius of maximum <sup>(a)</sup> wind speed, $R_{max}$ (km)	Lognormal	$\lambda = 3.995$ $\zeta = 0.275$	$\lambda = \ln(260/\sqrt{\Delta p})$ $\zeta = 0.461$	$\lambda = 4.045 - 0.0083\Delta p$ $\zeta = 0.451$	$\lambda = 3.984 - 0.012\Delta p$ $\zeta = 0.350$
Translation velocity, $V_t$ (m/s)	Lognormal	$\lambda = 1.787$ $\zeta = 0.513$	$\lambda = 1.805$ $\zeta = 0.456$	$\lambda = 1.616$ $\zeta = 0.365$	$\lambda = 1.734$ $\zeta = 0.418$
Filling constant, $a$	Normal	$\mu = 0.032$ $\sigma = 0.025$	$\mu = 0.042$ $\sigma = 0.016$	$\mu = 0.021$ $\sigma = 0.014$	$\mu = 0.024$ $\sigma = 0.033$

<sup>(a)</sup> The different forms of the distribution parameter  $\lambda$  reflect the marginal correlation between radius of maximum winds and central pressure difference.

Huang 1999), a decay model having the following form was assumed in the present study:

$$\Delta p(t) = \Delta p_0 \exp(-at) \quad (1)$$

where  $\Delta p(t)$  = the difference between the central pressure and the atmospheric pressure at a distance beyond the effect of the hurricane at time  $t$ ;  $\Delta p_0$  = the pressure difference when the hurricane crossed the coast;  $a$  is the filling constant modeled as a normally distributed random variable. The mean and standard deviation of the filling constant  $a$  for the three states investigated (North Carolina, South Carolina and Florida) are shown in Table 1. This decay (filling) model is similar to that used by Vickery and Twisdale (1995), however their model suggests a more rapid filling rate for most of the hurricanes considered. In this study, the correlation between the filling rate and the intensity of the storm was also found to be statistically insignificant. Further information on the decay model may be found elsewhere (Huang *et al.* 1998, Huang 1999).

Probabilistic process models were used in the event-based Monte Carlo simulations in this study. Specifically, the occurrence of hurricanes was modeled as a Poisson process while a Markov chain was used to model the state changes of a hurricane. The basic concept of Monte Carlo simulation is the direct sampling from the distributions of all the random variables considered. Since the generation of random variables is a relatively simple task, Monte Carlo techniques can be used to simulate discrete and continuous random processes. Simulation therefore provides a framework for considering spatial uncertainty and temporal uncertainty simultaneously, i.e., a time-dependent analysis. Using event-based hurricane simulation as an example, the realizations in the time domain are generated first (i.e., hurricanes are generated according to an arrival model). Then, realizations of the random variables defining the gradient wind field are generated in the space domain. Using appropriate surface-to-gradient conversion factors, the surface wind speeds can also be determined. The hurricane is then moved to the next location and the wind field is re-generated taking into account spatial changes such as decay. After the hurricane has degraded to the point that wind speeds are no

longer significant, the simulation proceeds to the next randomly generated hurricane event. These steps are repeated a specified number of times, and the distributions of maximum wind speeds (e.g.,) are determined. Again, since the simulation procedure is not the focus of this paper, the interested reader is referred elsewhere for further discussion about Monte Carlo simulation and its application to hurricane simulation (Huang *et al.* 1998, Huang 1999).

Five basic variables were used to characterize the wind field in this study: central pressure difference ( $\Delta P$ ), radius of maximum winds ( $R_{max}$ ), approach angle ( $\theta$ ), translation velocity ( $V_t$ ) and annual occurrence rate ( $\lambda$ ). These event model parameters were determined from an analysis of historical landfalling hurricanes in the region of interest (Huang *et al.* 1999). Hurricane data covering 112 years (1887-1998) were used to determine the distribution and statistical moments (including possible correlations) of the five basic variables. Three states (North Carolina, South Carolina, and Florida) in the Southeastern United States were investigated, each having site-specific statistical information (see Table 1). Since hurricanes can approach the Florida peninsula from either the Atlantic Ocean or the Gulf of Mexico, two sets of statistics were developed to model the characteristics of hurricanes approaching from each of these directions. The transition matrix for the Markov analysis was developed using historical hurricane track information which reported the storms position every six hours (Neuman *et al.* 1997). The translational wind speed states in the transition matrix therefore corresponded to the ratios of current states to the translational wind speed at landfall at each six-hour interval. The simulated results were shown to agree well with actual data. Further details and discussion of this procedure can be found elsewhere (Huang 1999, Huang *et al.* 1999).

The previous section was provided as background to the present study. The next three sections focus specifically on the analysis of directionality effects on wind loads on low-rise structures.

### 3. Directionality effects due to atmospheric flow patterns

The states of South Carolina (SC) and Florida (FL), both located in the southeastern United States, are used to illustrate the procedure to evaluate directionality effects due to atmospheric flow patterns. To eliminate the effects of local exposure on wind climate directionality, all sites considered are assumed to be located in the middle of an ordinary commercial airport (open terrain). The surface wind speeds (10-minute mean and 3-second gust) are assumed to be at a standard height of 10 m. The 50-year maximum gradient, as well as the 10-minute mean and 3-second surface gust wind speeds, occurring in each of the 16 azimuths are recorded for each simulation. The overall (direction independent) maximum gradient, and mean and gust surface wind speeds, are also recorded. The maximum wind speed values (wind speeds at each azimuth and overall direction-independent maximum speed) from 1000 simulated 50-year exposure periods were used to evaluate the  $N$ -year mean recurrence interval (MRI) wind speeds, defined as wind speeds having an annual exceedance probability of  $1/N$ , at the sites investigated. Since the mean annual occurrence rates for the states of South Carolina and Florida are taken as 0.306 and 0.631, respectively (see Table 1), about 15,000 hurricane events were simulated for South Carolina and about 31,500 hurricane events were generated for Florida. Several sites, including Charleston, SC, Columbia, SC, Miami, FL, Orlando, FL, and Panama City, FL are used in this study to characterize wind climate directionality in the southeastern United States. The locations of these five sites are shown in Fig. 1.

In developing directional MRI wind speeds, the issue of correlation has frequently been of some concern. Note that the event-based simulation approach herein, in which events and their tracks are generated according to prescribed random variables/processes, implicitly takes into account correlation



Fig. 1 Selected sites in the southeastern United States

in the directional maxima. That is, this approach permits the possibility that one particular event results in the  $m$ -year maximum wind speed in more than one direction. Recall that in each simulation, the maximum wind speed in each direction is recorded, as is the overall (direction-independent) wind speed. In general, the simulation does not keep track of the specific event causing the  $m$ -year maximum wind speed for each direction; however, when modified to do so, it was found that the correlation coefficient  $r$  (pairwise correlation between adjacent directions) was between 0.5 and 0.6. How to account for this correlation in the selection of directionality factors for design, however, remains to be addressed.

Assuming independent annual maximum wind speeds, the probability of exceeding the  $N$ -year MRI wind speed in  $m$  years is  $1-(1-(1/N))^m$ . Thus, the knowledge of the  $m$ -year maximum wind speed distribution could also be used to evaluate the  $N$ -year MRI wind speeds. The 50-year, 100-year, 500-year, and 1000-year MRI's for the sites investigated are obtained from the 1000 50-year maximum wind speed values (including overall maximum wind speeds and maximum wind speeds for each direction). The wind speed (or wind load) directionality factor is defined herein as the ratio of the  $N$ -year MRI wind speed (or wind load) in each direction divided by the non-directional  $N$ -year MRI wind speed (or wind load). The wind speed and wind load directionality factors are of course different, since the load on low-rise structures is taken as proportional to the square of the velocity. Note that the directionality factor cannot be greater than one because the directional  $N$ -year MRI is by definition less than or equal to the non-directional  $N$ -year MRI. This definition of directionality factor offers some advantage. By normalizing the directional MRI's by the non-directional MRI's (i.e., code values), the results from the present study can readily be applied to

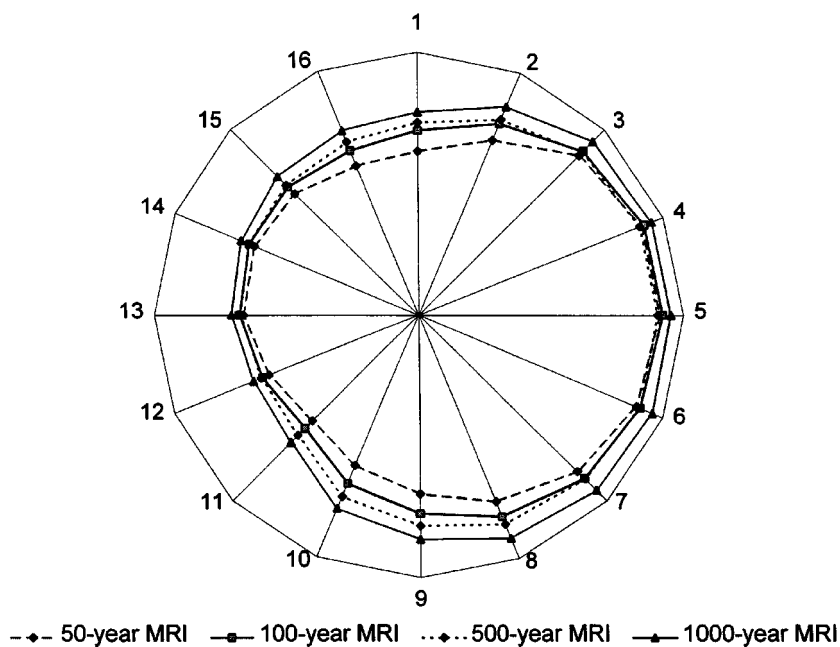


Fig. 2 Wind speed directionality factors for Charleston, SC

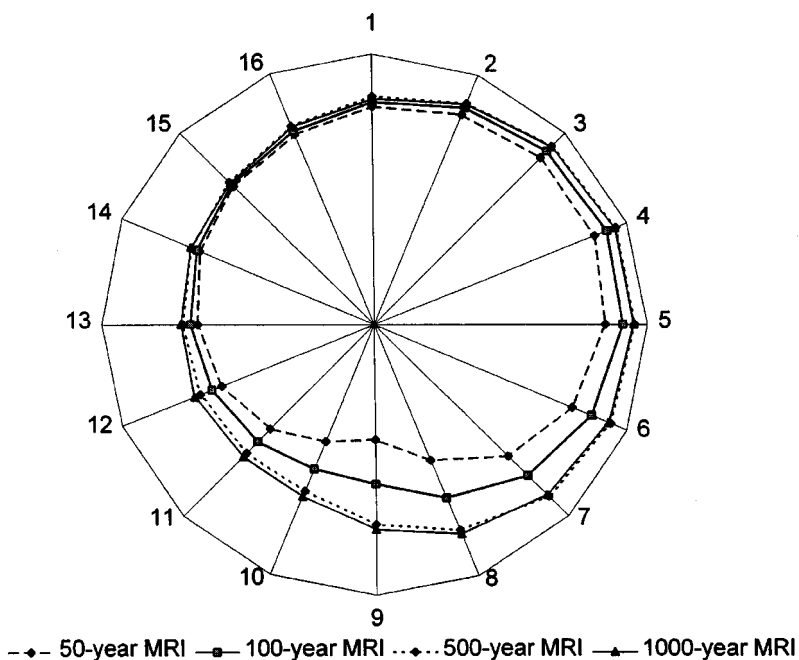


Fig. 3 Wind speed directionality factors for Columbia, SC

areas having a similar wind climate and which are located a similar distance from the coast. For example, the design wind speed (50-year MRI gust wind speeds) for Charleston in ASCE 7-95 is

53.6 m/s. The design wind speed for each direction can be obtained by multiplying this value by the 50-year MRI directionality factor for each direction at Charleston. (This is true even though the 50-year MRI gust wind speed in ASCE 7-95 differs from that obtained in the present study.) The same directionality factor can also be applied to Wilmington, NC, which has a similar wind climate to Charleston and which is also located 10-15 km from the coast. A similar directionality factor analysis is performed for the other sites considered in this study. Fig. 2 and 3 show the results for Charleston and Columbia, respectively. Charleston represents a site about 10 km from the coast, while Columbia represents a site located more than 150 km inland. The results for all the five sites investigated are shown in Table 2.

As seen in Fig. 2 and 3 and the results shown in Table 2, the directionality factor varies with direction. These results further suggest the directionality factor depends on the relative distance from the coast as well as the wind climate in that region. In general, for sites near the coast (such as Charleston, Miami, and Panama City), the directionality factor is controlled by the orientation of the site relative to the coast. That is, the directions toward the water (i.e., wind coming from the ocean) have larger directionality factors than those facing inland. As a hurricane moves inland after making landfall, it generally takes 10-15 km before the over-water gust structure at 10 m changes to an over-land gust structure (Sparks and Huang 1999). Therefore, the wind blowing from the water to the land will be much stronger than the wind blowing from the land to the water, resulting in larger directionality factors when the wind is coming off the water. For inland sites, such as Columbia and Orlando, the directionality factor is more a function of the decay (filling) rate of the hurricane. Since hurricanes are modeled in this study simply as translating vortices with counter-clockwise rotation in the Northern Hemisphere, the wind is stronger as the storm approaches a site than as it leaves (due to decay in intensity). Therefore, the north-to-east directions (directions 1-5 in Fig. 3)

Table 2 Directionality factors for the sites investigated

	Charleston				Columbia				Miami				Orlando				Panama City			
Dir.	MRI (years)				MRI (years)				MRI (years)				MRI (years)				MRI (years)			
	50	100	500	1000	50	100	500	1000	50	100	500	1000	50	100	500	1000	50	100	500	1000
N	0.63	0.70	0.73	0.77	0.81	0.82	0.84	0.83	0.64	0.77	0.87	0.88	0.82	0.86	0.90	0.90	0.68	0.71	0.78	0.78
NNE	0.72	0.79	0.81	0.86	0.84	0.87	0.89	0.89	0.85	0.89	0.93	0.93	0.88	0.90	0.94	0.95	0.75	0.79	0.84	0.85
NE	0.86	0.88	0.88	0.94	0.87	0.90	0.93	0.93	0.93	0.95	0.97	0.96	0.93	0.94	0.97	0.96	0.80	0.84	0.87	0.89
ENE	0.91	0.92	0.90	0.95	0.87	0.92	0.96	0.95	0.95	0.96	0.97	0.98	0.93	0.95	0.97	0.97	0.82	0.86	0.89	0.89
E	0.91	0.92	0.90	0.95	0.85	0.91	0.95	0.95	0.93	0.94	0.96	0.96	0.93	0.94	0.97	0.97	0.83	0.85	0.88	0.89
ESE	0.89	0.91	0.91	0.96	0.79	0.86	0.94	0.93	0.89	0.91	0.95	0.95	0.89	0.91	0.95	0.95	0.92	0.94	0.96	0.97
SE	0.84	0.88	0.88	0.94	0.69	0.79	0.90	0.89	0.84	0.87	0.92	0.92	0.84	0.86	0.91	0.92	0.90	0.91	0.93	0.92
SSE	0.77	0.83	0.86	0.92	0.54	0.69	0.82	0.83	0.81	0.83	0.88	0.89	0.79	0.81	0.86	0.87	0.86	0.88	0.89	0.89
S	0.68	0.76	0.80	0.86	0.43	0.59	0.74	0.76	0.77	0.78	0.83	0.83	0.76	0.79	0.83	0.85	0.83	0.86	0.86	0.86
SSW	0.62	0.70	0.75	0.80	0.47	0.58	0.67	0.69	0.71	0.72	0.74	0.75	0.75	0.78	0.82	0.83	0.82	0.84	0.85	0.85
SW	0.57	0.61	0.65	0.68	0.54	0.61	0.67	0.69	0.71	0.72	0.74	0.74	0.75	0.78	0.81	0.81	0.78	0.81	0.83	0.84
WSW	0.61	0.64	0.64	0.67	0.61	0.64	0.69	0.71	0.69	0.71	0.73	0.73	0.74	0.77	0.80	0.81	0.76	0.78	0.82	0.83
W	0.66	0.68	0.67	0.71	0.65	0.68	0.70	0.71	0.64	0.68	0.72	0.73	0.74	0.76	0.81	0.81	0.74	0.77	0.81	0.82
WNW	0.67	0.69	0.70	0.73	0.69	0.70	0.73	0.73	0.57	0.65	0.72	0.72	0.75	0.77	0.82	0.81	0.66	0.69	0.75	0.75
NW	0.66	0.69	0.70	0.75	0.72	0.73	0.75	0.74	0.52	0.61	0.72	0.73	0.76	0.80	0.83	0.84	0.65	0.68	0.74	0.74
NNW	0.61	0.68	0.71	0.76	0.76	0.77	0.79	0.79	0.50	0.61	0.74	0.76	0.79	0.82	0.86	0.87	0.64	0.67	0.73	0.75

will experience higher wind speeds and therefore higher directionality factors in cases where hurricanes approach from the east. However, for those sites along the west coast of Florida, the directionality factors are higher in the east-to-south directions (directions 5-9) since the highest winds generally result from storms approaching from the west at those locations. Note that since hurricanes can approach Orlando (an inland Florida location) from either coast, the directionality factor for Orlando is more uniform than that for Columbia (an inland South Carolina location), a site at which most hurricanes come from the east. For both coastal sites and inland sites, the directionality factor increases (approaching one) as the MRI increases. For the 1000-year MRI, for example, the maximum directionality factor for each site is nearly one. Moreover, as the MRI gets larger, the directionality factor becomes more uniform in all directions.

#### 4. Directionality effects due to local exposure

It is unlikely that many buildings will be sited in the middle of an airport having standard open terrain. The effects of realistic terrain, exposure, and sheltering on the resulting wind loads on structures may be significant. It may therefore be of interest to try to account for local exposure effects (siting effects such as shielding, orientation, etc.) in design. To account for these effects with a directionality adjustment, the factor described above for open terrain would need to be transformed to other terrains/exposures. Thus, a “local” directionality factor might be introduced which can effectively combine these two adjustments (*event* directionality and *siting* or *local exposure* directionality). While information may not yet be available to make such an approach practical or even possible, the concept is discussed and illustrated here.

The adjustment of the directionality factor to a “local” factor is a function of the local exposure effects on the vertical wind profile, i.e., the ratios of the gradient-to-surface conversion factor for the local exposure to those for open terrain. In the simulation to characterize the wind directionality for open terrain, gradient-to-gust conversion factors of 0.90 and 0.80 were used for sites located directly on the beach and within 10 km of the coast, respectively, when the wind is blowing from the water to the land. When the wind is blowing from the land to the water (with increased surface roughness), the conversion factors change to 0.80 and 0.72, respectively. For inland sites, the gradient-to-gust conversion factor is 0.72 regardless of wind direction. Similarly, the gradient-to-mean conversion factors are 0.65 and 0.50 for sites located directly on the beach and open sites, respectively, at initial landfall with wind blowing from the water; 0.50 and 0.45, respectively, with wind blowing from the land; and 0.45 for open sites located far inland regardless of wind directions. The bases for all of these conversion factors are provided in (Huang *et al.* 1999). Therefore, some knowledge of local exposure (i.e., the gradient-to-surface conversion factor) and directionality factor for that site assuming open terrain is needed to determine the local directionality factor.

As an illustrative example of the effects of local exposure on wind speed directionality, consider a building on a fictitious site near Columbia, SC (see Fig. 4). This building is assumed to be located near a large lake. Therefore, a near over-water wind-profile is assumed to develop when the wind is blowing from the lake to the shore. A gradient-to-gust conversion factor of 0.85 is taken to represent the local exposure. The area to the east of the structure is heavily wooded while the areas to the north and south are grassland (similar to open terrain). When the wind blows from the direction of the trees, a gradient-to-gust conversion factor of 0.60 is assumed (to account for shielding effects from the trees). For wind coming over the grassland, the local exposure is assumed to be similar to open terrain with a gradient-to-gust conversion factor of 0.72. With this information, the directionality



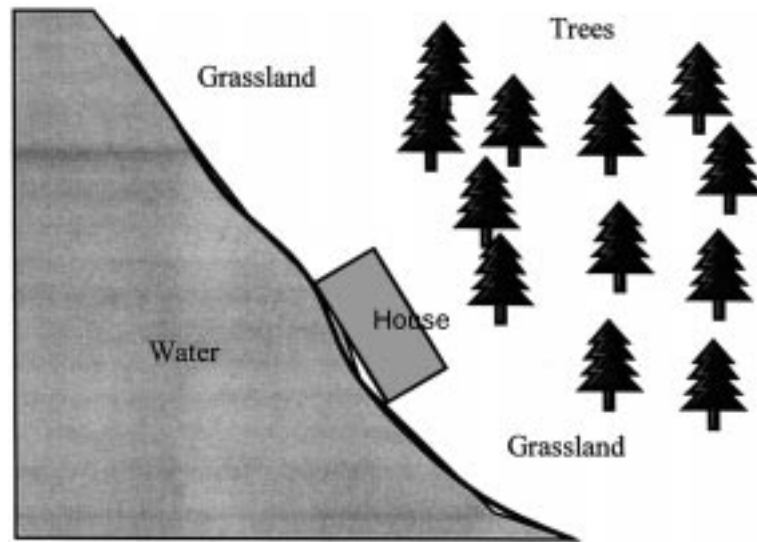


Fig. 4 Local exposure of an illustrative site near Columbia, SC

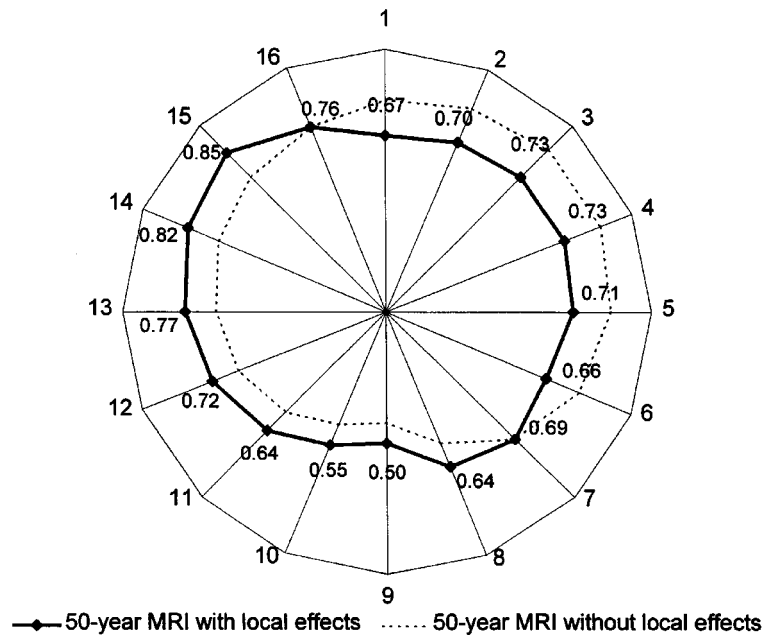


Fig. 5 Wind speed directionality factors (50-year MRI) considering local exposure

factor plot for Columbia without consideration of local effects (Fig. 3) can be modified to account for local exposure using a modification factor ( $\gamma$ ). When the wind is blowing from the lake,  $\gamma = 0.85/0.72 = 1.18$ ; when the wind is blowing from the direction of the woods,  $\gamma = 0.60/0.72 = 0.83$ ; for other directions,  $\gamma = 0.72/0.72 = 1.00$ . The resulting directionality factors (for a 50-year MRI) considering local exposure are shown in Fig. 5. Also shown are the 50-year MRI directionality

factors without consideration of local effects. Due to the increased wind speeds from the open water and decreased wind speeds from the direction of the trees, the maximum directionality factor shifts in the presence of these geographic features from a northeast direction to a northwest direction. Note that since the modification factor can be greater than one, the product of the modification factor and the directionality factor for open terrain could also be greater than one. The same modification factors can be applied to other MRI's since the modification factor is only a function of local exposure and is independent of the statistical extreme wind climate.

## 5. Directional and non-directional bases for design wind speeds

### 5.1. Directional method

In this study, the concept of an equivalent wind speed is used when considering wind load directionality effects. This is compatible with the method presented by Simiu and Heckert (1998). We assume the wind effect  $Q(\theta)$  can be described by the following expression:

$$Q(\theta) = \frac{1}{2}\rho C(\theta)U^2(\theta) \quad (2)$$

where  $\rho$  = air density,  $C(\theta)$  = aerodynamic pressure coefficient corresponding to wind blowing from direction  $\theta$ , and  $U(\theta)$  = wind speed. A set of  $N$  time series of wind loads can be formed according to the following equation:

$$Q_j(\theta_i) = C(\theta_i)U_j^2(\theta_i)/\max(C(\theta_i)) \quad (3)$$

where  $i = 1, 2, \dots, N$  denotes the direction and  $j = 1, 2, \dots, M$ , where  $M$  denotes the number of hurricane events. Note that the wind load has been normalized by the maximum aerodynamic pressure coefficient. Then, a single time series of equivalent wind speeds can be obtained as:

$$U_{j,eq} = \sqrt{\max(Q_j(\theta_i))} \quad (4)$$

The analysis of the equivalent wind speeds yields the extreme value  $U_{R,eq}$ , where  $R$  denotes the MRI. Accordingly, the wind effect having the same MRI can be expressed using Eqs. (3) and (4) as:

$$Q_R = (\rho/2)\max(C(\theta_i))U_{R,eq}^2 \quad (5)$$

### 5.2. Non-directional method

Using non-directional methods, the time series of maximum wind speeds in all directions (i.e., direction-independent) are analyzed to find the extreme wind speed  $U_R$ . The wind load ( $Q_{R,nom}$ ) is then determined as a function of the maximum direction-independent aerodynamic pressure coefficient and the extreme wind speed  $U_R$ :

$$Q_{R,nom} = (\rho/2)\max(C(\theta_i))U_R^2 \quad (6)$$

Note that the wind load calculated using this method will not have the same MRI as the extreme wind speed. It is therefore considered a nominal MRI wind load (Simiu and Heckert 1998). Since

$U_j \geq U_{j,eq}$ , it follows that  $Q_{r,nom} \geq Q_R$ . Therefore, the non-directional method will result in conservative design wind loads. However, as will be shown later, the degree of conservatism decreases as the MRI increases.

### 5.3. Simulation results and discussion

Direction-dependent wind loads are evaluated herein using the direction-specific aerodynamic coefficients given by Peterka and Cermak (1978). This allows for direct comparison with the study by Simiu and Heckert (1998). The aerodynamic coefficients corresponding to a corner location on the roof of a tall building are listed in Table 3. For illustrative purposes and simplicity, we assume the roof has a height of 10 m. While these coefficients were determined for the roof of a tall building, this assumption (made for illustrative purposes) ensures that uncertainties associated with the vertical wind profile adjustment are not introduced into the simulation. Otherwise, the choice of these coefficients is fairly arbitrary. In each direction, time series are recorded for wind speed, wind load, and equivalent wind speed, as defined previously. The wind load time series is used to analyze the directionality of wind load and the influence of aerodynamic coefficient on wind load directionality. The equivalent wind speed series is used to analyze the conservatism of the non-directional method. Since the aerodynamic coefficients given by Peterka and Cermak correspond to hourly mean speed, a gust factor for inland open terrain of 1.6 (Sparks and Huang 1999) is applied to the simulated gust wind speeds for each direction. The square of these values are then multiplied by the aerodynamic

Table 3 Direction-dependent aerodynamic coefficient (from: Peterka and Cermak 1978)

$\theta_i$	N	NNE	NE	ENE	E	ESE	SE	SSE	S	SSW	SW	WSW	W	WNW	NW	NNW
$C(\theta_i)$	1.1	1.0	0.5	0.6	0.7	0.6	0.5	0.9	1.8	3.3	1.1	0.6	0.1	0.2	0.2	0.8

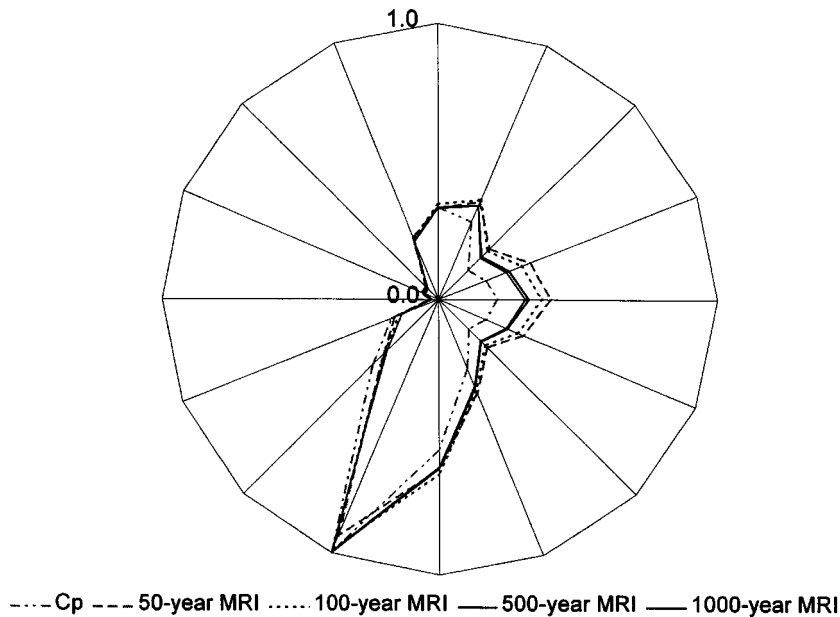


Fig. 6 Wind load directionality factor for Charleston, SC

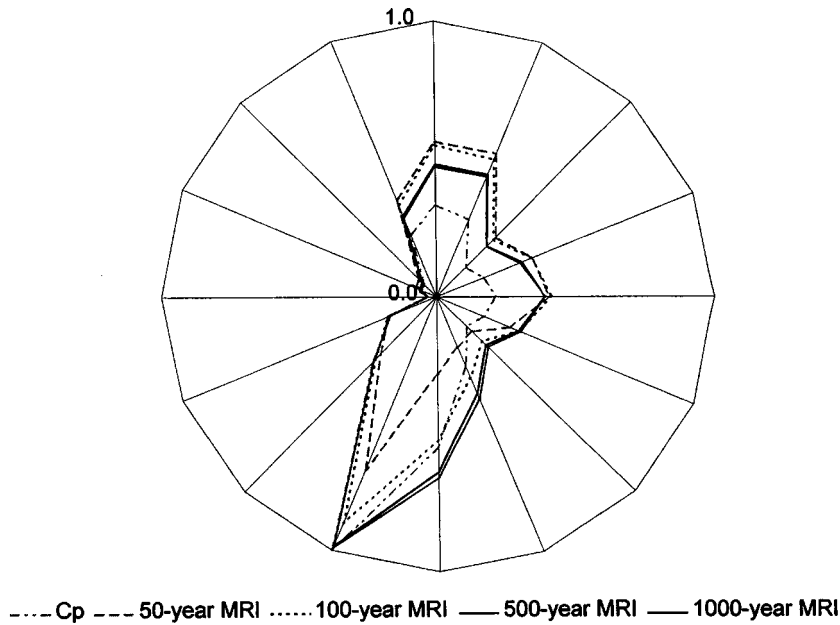


Fig. 7 Wind load directionality factor for Columbia, SC

coefficients to obtain the wind loads. The equivalent hourly mean wind speed is then obtained using Eq. (4) and the maximum wind loads in all directions. This is then multiplied by the gust factor of 1.6 to determine the equivalent gust wind speeds.

Figs. 6 and 7 show the wind load directionality factor along with the normalized aerodynamic pressure coefficient ( $C(\theta_i)/\max(C(\theta_i))$ ) in each direction for Charleston and Columbia, respectively. The directionality factors corresponding to the 50-year, 100-year, 500-year, and 1000-year MRI wind loads are shown on these figures. The normalized aerodynamic pressure coefficients are also shown on these figures. As with the directionality factor for wind speed, the wind load directionality factor is less than one and increases (toward unity) with increasing MRI. However, the rate of increase of directionality factor with MRI is greater than that for wind speed. The wind load directionality factor is not as uniform (i.e., the contour is not as circular) as that for wind speed and is controlled by the shape of the normalized aerodynamic pressure coefficient (see Figs. 6 and 7).

Fig. 8 shows the ratio of equivalent MRI wind speed to the MRI wind speed ( $r_R = U_{R,eq}/U_R$ ) as a function of MRI for Charleston. The ratio increases with MRI, indicating the decrease in conservatism that results from neglecting directionality effects as the mean recurrence interval (MRI) increases. Similar results can be obtained for other sites using the same aerodynamic pressure coefficients. For short MRI's, however, the degree of conservatism can be significant. For example, the ratio  $r_R$  is about 0.66 for a 50-year MRI. This suggests that the directional load having a 50-year MRI is only about 44% ( $0.66^2$ ) of the direction-independent design load. For a 500-year MRI, the directional load is about 59% ( $0.77^2$ ) of the direction-independent design load. In ASCE 7-95, a directionality factor of 0.85 (which is embedded in the load factor of 1.3) is assumed to account for the reduced probability that the direction of the maximum wind speed will coincide with the least favorable building orientation (i.e., worst-case aerodynamic pressure coefficients). Based on the simulation results in the present study (factors of 0.44 and 0.59 for 50-year and 500-year MRIs, respectively),

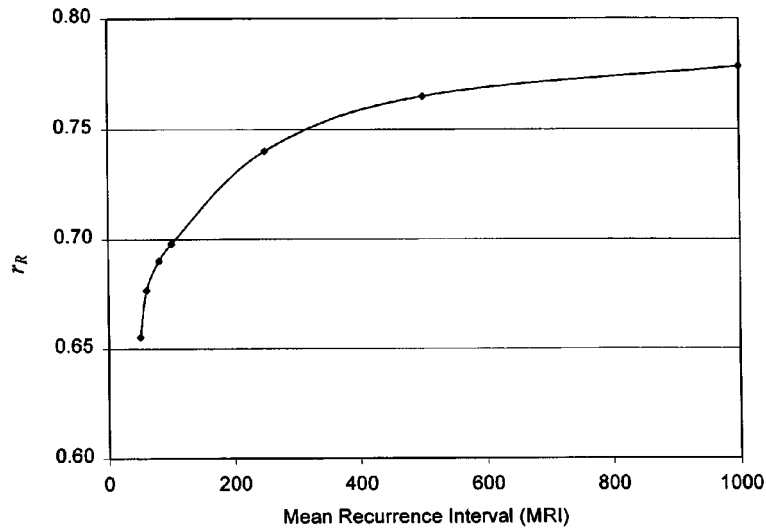


Fig. 8 Ratio ( $r_R$ ) of equivalent wind speed to nominal wind speed as a function of MRI

this factor of 0.85 would appear conservative for most cases. There are two cases worth noting, one for which the directionality factor is not relevant, and the other for which the directionality factor may approach one. If the wind climate directionality and the aerodynamic pressure coefficients are relatively uniform (i.e., near direction-independent), the issue of directionality in wind speeds (loads) is not relevant. In the other case, if the directions corresponding to maximum winds and aerodynamic pressure coefficients coincide (which is the worst-case scenario assumed by Simiu and Heckert 1998), the directionality factor may approach one. However, the probability of this latter situation occurring is relatively low. Therefore, in general, the design loads obtained using the non-directional method will be higher than those obtained using directional methods.

In a recent paper on directionality effects in non-hurricane and hurricane-prone regions, Simiu and Heckert (1998) concluded that the favorable effect of wind directionality tends to be marginal for mean recurrence intervals associated with ultimate wind loads. This is true under certain conditions (such as the worst-case scenario mentioned earlier) and for extremely large MRI's, i.e., more than 100,000 years (Simiu and Heckert 1998). Even though in some cases, ultimate design wind loads may have recurrence intervals of more than 500 or 1000 years, discussing MRI's greater than 1000 years has little practical meaning, since buildings generally are not designed to withstand such extreme events. Furthermore, we have little confidence in predicting extreme events having such long recurrence intervals. Simiu and Heckert (1998) correctly point out that the estimated extreme wind speeds having very long mean recurrence intervals are unreliable. Therefore, results based on the analysis of very large MRI's can not be viewed as conclusive. Theoretically, since  $U_j \geq U_{j,eq}$  for any given time series, the value of  $r_R$  at any site cannot be greater than one. However, in the paper by Simiu and Heckert (1998), values for  $r_R > 1$  for very long recurrence intervals (e.g.,  $R = 100,000$  years) are suggested. This contradiction calls into question the ability to accurately estimate wind speeds having very long recurrence intervals as well as the finding of only marginal conservatism for large MRI's. Moreover, the simulation results from the present study indicate that design loads obtained using non-directional methods are still conservative even for MRI's as large as 1000 years.

## 6. Conclusions

This paper presents an approach for evaluating directionality effects for both wind speeds and wind loads on low-rise structures in hurricane-prone regions. Using event-based simulation, hurricane directionality effects are determined for an open-terrain condition at various locations in the southeastern United States. The wind speed (or wind load) directionality factor, defined as the ratio of the  $N$ -year mean recurrence interval (MRI) wind speed (or wind load) in each direction to the non-directional  $N$ -year MRI wind speed (or wind load), is greater than one and increases toward unity with increasing MRI. Thus, the degree of conservatism that results from neglecting directionality effects decreases with increasing MRI. The main conclusions from this study are as follows:

- 1) Wind load directionality effects on structures are combined effects resulting from atmospheric flow pattern, local exposure, and aerodynamic pressure coefficients. Separating these effects enables the results from the present study to be extended to other sites.
- 2) In general, the use of non-directional methods to determine design wind loads (such as those found in most load standards) is conservative. However, the degree of conservatism decreases as the mean recurrence interval increases.
- 3) Limited confidence can be placed on statements about the conservatism of non-directional methods to determine wind speeds with very large MRI's (i.e., more than 1000 years).

It may be desirable to account for local exposure effects (siting effects such as shielding, orientation, etc.) in design. To account for these effects in a directionality adjustment, the factor described above for open terrain would need to be transformed to other terrains/exposures. A "local" directionality factor, therefore, must effectively combine these two adjustments (*event* directionality and *siting* or *local exposure* directionality). By also considering the direction-specific aerodynamic coefficient, a direction-dependent wind load can be evaluated. While the data necessary to make predictions of directional wind loads may not routinely be available in the case of low-rise structures, the concept is discussed and illustrated in this paper.

## Acknowledgements

Funding for this study was provided by the South Carolina Sea Grant Consortium. The authors gratefully acknowledge this support.

## References

- ASCE (1995), *Minimum Design Loads for Buildings and Other Structures*, ASCE 7-95, American Society of Civil Engineers, New York, NY.
- Batts, M.E., Cordes, M.R., Russell, L.R., Shaver, J.R. and Simiu, E. (1980), *Hurricane Wind Speeds in the United States*, NBS Building Science Series 124, U.S. Department of Commerce, National Bureau of Standards, Washington, DC.
- Davenport, A.G. (1977), "Prediction of risk under wind loading", *Proceedings of 2nd International Conference on Structural Safety and Reliability* (ICOSSAR), Munich, Germany, 511-538.
- Georgiou, P.N. (1985), *Design Wind Speeds in Tropical Cyclone-Prone Regions*, Ph.D. Dissertation, Department of Civil Engineering, University of Western Ontario, Canada.
- Huang, Z. (1999), *Stochastic Models for Hurricane Hazard Analysis*, Ph.D. Dissertation, Department of Civil Engineering, Clemson University, Clemson, SC.

- Huang, Z., Rosowsky, D.V. and Sparks, P.R. (1998), "Probability-based wind field modeling in GIS", *Proceedings of International Conference on GIS Applications in Environmental Modeling*, Hong Kong, June 1998.
- Huang, Z., Rosowsky, D.V. and Sparks, P.R. (1999), "Event-based hurricane simulation for the evaluation of wind speeds and expected insurance losses", *Proceedings of 10<sup>th</sup> International Conference on Wind Engineering*, Copenhagen, Denmark, 1417-1424.
- Neuman, C.J., Jarvinen, B.R., McAdie, C.J. and Elms, J.D. (1997), *Tropical Cyclones of the North Atlantic Ocean, 1871-1992*, U.S. Department of Commerce NOAA.
- Peterka, J.A. and Cermak, J.E. (1978), *Wind-Tunnel Study of Atlanta Office Building*, Department of Civil Engineering, Colorado State University, Fort Collins, CO.
- Rosowsky, D.V., Huang, Z. and Sparks, P.R. (2000), "Long-term risk assessment and expected damage to residential structures", *Reliability Engineering & System Safety* (special issue on risk assessment of engineering facilities), to appear.
- Russell, L.R. (1968), *Probability Distributions for Texas Gulf Coast Hurricane Effects of Engineering Interest*, Ph.D. Dissertation, Stanford University, Stanford, CA.
- Russell, L.R. (1971), "Probability distributions for hurricane effects", *ASCE Journal of Waterways, Harbors, and Coastal Engineering*, **97**(1), 139-154.
- Simiu, E. and Filliben, J.J. (1981), "Wind direction effects on cladding and structural loads", *Engineering Structures*, **3**, 181-186.
- Simiu, E. and Heckert, N.A. (1998), "Ultimate wind loads and direction effects in non-hurricane and hurricane-prone regions", *Environmetrics*, **9**, 433-444.
- Simiu, E. and Scanlan R.H. (1996), *Wind Effects on Structures*, John Wiley & Sons, New York.
- Sparks, P.R. and Huang, Z. (1999), "Wind speed characteristics in tropical cyclones", *Proceedings of 10<sup>th</sup> International Conference on Wind Engineering*, Copenhagen, Denmark.
- Tryggvason, B.V., Surry, D. and Davenport, A.G. (1976), "Predicting wind-induced response in hurricane zones", *ASCE Journal of Structural Division*, **102**(12), 2333-2350.
- Tuleya, R.E., Bender, M.A. and Kurihara, Y. (1984), "A simulation study of the landfall of tropical cyclones using a movable nested-mesh model", *Monthly Weather Review*, **112**(1), 124-136.
- Vickery, P.J. and Twisdale, L.A. (1995), "Prediction of hurricane wind speeds in the united states", *ASCE Journal of Structural Engineering*, **121**(11), 1691-1699.
- Wen, Y.K. (1983), "Wind direction and structural reliability", *ASCE Journal of Structural Engineering*, **109**(4), 1028-1041.
- Wen, Y.K. (1984), "Wind direction and structural reliability: II", *ASCE Journal of Structural Engineering*, **110**(6), 1253-1264.

( Communicated by Jun Kanda )